Journal of Clinical and Medical Images

Research Article

ISSN: 2640-9615 | Volume 6

Head-To-Head Comparison of Lesion Detection and PET Metrics on 18F-FDG PET/CT and PET/MR in Hepatic Metastases

Levine C[1], Talmon Y[1], Kesler M[1], Kuten J[1] and Even-Sapir E[1,2*]

[1]Department of Nuclear Medicine, Tel Aviv Sourasky Medical Center, 6 Weizmann St., Tel Aviv 6423906, Israel

[2]Sackler School of Medicine, Tel Aviv University, Tel Aviv 6997801, Israel

[*]Corresponding author:

Einat Even-Sapir, MD.
Department of Nuclear Medicine, Tel Aviv Sourasky Medical Center, 6 Weizmann St., Tel Aviv 6423906, Israel. Tel: +97236973536, fax: +97236973895,
E-mail: evensap@tlvmc.gov.il

Received: 20 Nov 2022
Accepted: 01 Dec 2022
Published: 10 Dec 2022
J Short Name: JCMI

Citation:

Even-Sapir E, Head-To-Head Comparison of Lesion Detection and PET Metrics on 18F-FDG PET/CT and PET/MR in Hepatic Metastases. J Clin Med Img. 2022; V6(20): 1-7

Keywords:

PET/CT; PET/MR; Liver; Metastases

ORCID: Charles Levine (-), Yael Talmon (-), Mikhail Kesler (0000-0003-0786-084X), Jonathan Kuten (0000-0002-3458-9904), Einat Even-Sapir (0000-0003-2487-0310).

1. Abstract

1.1. Purpose: This study is a comparison of performance of PET/CT vs PET/MR evaluation of hepatic metastases, comparing PET metrics and hepatic lesion identification.

1.2. Methods: Comparison of liver lesions and PET metrics of PET/CT and PET/MR were performed in 24 oncologic patients, with 191 hepatic metastases were identified utilizing MR. Lesions were evaluated for visibility on PET, as well as for comparison of PET metrics.

1.3. Results: PET of PET/CT missed 58/191 lesions (29%), and PET of PET/MR missed 45/191 lesions (24%). Of 109 lesions smaller than 2.5 cm, PET of PET/CT missed 50/109 (46%) lesions and PET of PET/MR missed 44/109 (40%) lesions ($p< 0.001$). Very strong correlation was noted between PET SUV and TBR values extracted from PET/MR and PET/CT images, with Pearson R values of .89 for SUVmean, .91 for SUVmax, .90 for TBRmean, and .93 for TBRmax. Bland-Altman plots demonstrated higher values of PET obtained on PET/MR. An average difference in measurement of SUV between PET/CT and PET/MR of 2.8 gr/ml for SUVmean (17.9%), and 4.8 gr/ml for SUVmax (23.1%) was noted. Similarly, for TBR higher measurements were shown for PET/MR, with an average difference of 1.9 for TBRmean (18.5%) and 1.1 for TBRmax (18.6%).

1.4. Conclusion: Improved visualization and uptake on PET of PET/MR, as well as the superiority of MR in detection of lesions make PET/MR a more sensitive modality for the detection of liver metastases, especially in cases of smaller lesions. These findings may impact accurate staging of liver disease and monitoring response to therapy.

2. Background

Liver is the second most common organ site of metastases, from a variety of primary tumors including lung, breast, and colon, and pancreas [1,2].

Accurate delineation of tumor spread in the liver is critical for optimizing treatment strategy. Different therapeutic options exist, with surgery representing the best chance for curative treatment, but with other options such as ablation, radiation, chemotherapy and novel biologic drugs or immunotherapy [3-5].

MRI of the liver is often considered to be the gold standard for evaluation of hepatic lesions [6]. MRI has a high sensitivity for hepatic lesions with a particular advantage over other modalities in evaluating smaller lesions, allowing for improved characterization and differentiating benign from malignant lesions [7].

PET/CT is commonly used for systemic oncologic imaging [8]. In addition to visualization of the lesions on CT, PET data yields important metabolic information. The combination of the two modalities offers complementary information. Likewise fusion of the PET with MR represents both ideal anatomic imaging of the liver

(MR), coupled with exquisite functional data (PET), improving diagnostic accuracy [9].

Recently it had become clear that morphologic data alone, such as the size of lesions, is insufficient to determine response to treatment. Use of PET scanning allows monitoring response using various metabolic tumor parameters [10]; these include SUV (standardized uptake value), MTV (metabolic tumor volume), TLG (total lesion glycolysis), and TBR (tumor to background ratio).

The purpose of the current study was head-to-head comparison of hepatic lesion detection and PET metrics on PET/CT and PET/MR in hepatic metastases.

3. Materials and Methods

Between January 2020 and February 2021, 24 oncologic patients with clinically or imaging suspected liver involvement gave written consent to have a PET/MR of the upper abdomen immediately following PET/CT acquisition. Nine patients gave such a consent twice during the course of the study, for a total of 33 exams. There were 13 male and 11 female patients, 37 to 81 years of age, and BMI from 19 kg/m2 to 37 kg/m2. The study was approved by the Institutional Review Board.

3.1. Imaging Protocol

All patients were injected with single dose of 5-6 Mbq/kg 18F-FDG. PET/CT acquisition began 50-90 min after injection and was immediately followed by PET/MR acquisition.

PET/CT studies were performed on the discovery MI PET/CT system (GE Healthcare) using automatic modulated current and 120 kV voltage. Images were reconstructed to 2.5mm slice thickness for diagnostic purposes and 3.75mm for AC purposes. Matrix size was 512x512. Oral and/or intravenous contrast material were given. 3D mode PET acquisition was performed at 2.5 min per bed. PET images were reconstructed by GE VUE Point FX algorithm is a fully 3D OSEM reconstruction including time of flight information.

PET/MR of the upper abdomen focused on the liver was performed soon after completion of the PET/CT. PET/MR was performed on an integrated PET/MR scanner (SIGNA™ PET/MR with QuantWorks - GE Healthcare), with a 5 detector array. Acquisition was initiated with 20 minutes PET acquisition time per bed position. All PET data for the PET/MR was reconstructed using time of flight information with 3D ordered subsets expectation maximization protocol iterative reconstruction algorithms. Reconstruction was performed in a similar manner to the PET/CT acquisition using GE VUE Point FX algorithm. A 3D T-1 weighted dual echo, RF spoiled sequence (LAVA-FLEX) in axial orientation was performed, generating 4 MRI images (water, fat, in phase, out phase) required to segment the image into 4 compartments: water, air, fat, and lung. Following segmentation, each pixel was assigned with 511 keV linear attenuation coefficients (LAR) allowing correction of PET signal attenuation.

MR evaluation included axial and coronal single shot FSE T2 weighted images, axial fast recovery FSE T2 weighted images with fat suppression, diffusion weighted images with ADC map, and axial Lava MPH T-1 fat suppression images before and after gadolinium, including arterial, portal and delayed phase imaging after gadolinium. Images were reviewed and analyzed with software provided by the manufacturer (AW workstation).

3.2. Image Analysis

Scan were interpreted jointly in consensus by a nuclear medicine physician (EES) and a body radiologist (CL) both with experience in oncologic imaging of PET/CT and PET/MR. PET/CTs were read on the Xeleris workstation, and PET/MRs were read using the GE AW workstation, reviewing the PET, CT, and MR, as well as fused images in the axial, sagittal, or coronal planes. Pathologic uptake in the liver was defined as focal uptake higher than that of background hepatic activity. MRI was utilized as a gold standard in defining the hepatic lesions to be evaluated.

The analysis began with the marking of volumes of Interest (VOIs) for liver lesions found in MR images. Next, rigid registration was done between PET of PET/CT images and PET of PET/MR images with manual fine tuning of the registration. The marked VOIs was then automatically copied from PET/MR image to the PET/CT image. Each VOI was carefully tested in all positions (axial, coronal and sagittal) to confirm it is properly located. Whenever it was necessary a fine manual adjustment was performed. Quantitative data was extracted using Q-Volumetrix application established in version V of the XELERIS platform by GE. Mean SUV (SUVmean) and maximum SUV (SUVmax) values were extracted for all lesions and were compared to SUV values of the background. Volume of interest (VOI's) of the background were marked in healthy liver tissue as manifested in all 4 modalities (PET of CT and PET of MR, CT and MR). Tumor-to-background ratio (TBR) including mean TBR (TBRmean) and maximum TBR (TBRmax) was obtained as well. Lesions with TBR of 1 or less were defined as not visualized on PET images.

3.3. Statistical Analysis

Detection rate of liver lesions by PET/CT and by PET/MR was compared, as were the quantitative PET data of PET obtained by PET/CT and by PET/MR. Three tests were used to establish agreement between PET/MR and PET/CT results: Bland-Altman test, paired t-test and Wilcoxon signed ranked test. Bland-Altman is a graphical representation of the differences between two assays as a function of the average values for each subject. The bias is estimated by the mean difference and limits of agreement are defined by 1.96 SD. Bland-Altman allows the identification of systematic error and outliers as well as the span of differences between the two methods of measurement. Paired t –test measure whether the mean difference between two depended variables is zero assuming the differences are normally distributed. Wilcoxon signed rank test is the non-parametric test equivalent to paired t-test where normal

distribution is not assumed.

Two correlation tests were applied; Pearson correlation and McNemar test. Pearson correlation is coefficient to measure correlation between two samples which is association between changes of the two variables. McNemar test measures the correlations between two binary nominal depended sets of data. It is used to find changes in the proportion of the paired data.

4. Results

A total of 191 liver lesions were identified on MR images. 58/191 lesions (29%) were not visible on PET images acquired using the PET/CT and 45/191 lesions (24%) were also not visible on PET images acquired using PET/MR. Of the 191 total lesions 109 lesions were defined as small (<2.5cm). The majority of lesions missed on both PET/CT and PET/MR were small lesions, however PET of PET/MR missed significantly less of these small lesions than PET of PET/CT with 50/109 (46%) lesions missed on PET/CT, and 44/109 (40%) missed on PET/MR, McNemar test, (P<0.001) (Figure 1).

Of the total of 191 lesions, 131/191 lesions were considered visible on both CT and MR and formed the basis of the comparison of PET metabolic data (SUV, TBR). PET (both CT and MR) SUV values ranged between 2 to 17 gr/ml for SUVmean, and 2.5 to 26 gr/ml for SUV max. There was moderate correlation between SUVmean and tumor size (R=0.5) and strong correlation of SUVmax to tumor size (R=0.7), (Pearson correlation, P<0.001).

Very strong correlation was noted between values extracted from PET/MR images and those extracted from PET/CT images both for SUV and for TBR. Pearson correlation calculated for each parameter is summarized in Table 1 (P<0.001). Correlation plots for SUV are presented in Figure 2 and 3.

Bland-Altman plots are presented in Figures 4-5 with numerical data summarized in Table 2. Limits of agreement in the Bland-Altman tests were defined in accordance with z-value corresponding to 95% confidence level for normal distribution. Overall, while the Bland-Altman plot also demonstrates good agreement between the PET/CT and the PET/MR, it also demonstrates that values of the PET/MR were consistently noted to be higher than on PET/CT. An average difference in measurement of SUV between PET/CT and PET/MR of 2.8 gr/ml for SUVmean (17.9%), and 4.8 gr/ml for SUVmax (23.1%) was noted. Similarly, for TBR higher measurements were shown for PET/MR, with an average difference of 1.9 for TBRmean (18.5%) and 1.1 for TBRmax (18.6%). The Bland-Altman plot also demonstrated that with increased average SUV the difference between PET of the MR and PET of the CT also increases (Figure 4 and 5).

Agreement between the two PETs quantitative parameters was also assessed using Wilcoxon signed ranked test and paired t-test. Both tests showed significant difference for all tested parameters between values extracted from PET/MR and those acquired from PET/CT with P<0.001. The tendency of PET/MR images to yield higher values is manifested in both tests. Paired t-test and Wilcoxon signed ranked test results are shown in table 3 and 4 correspondingly.

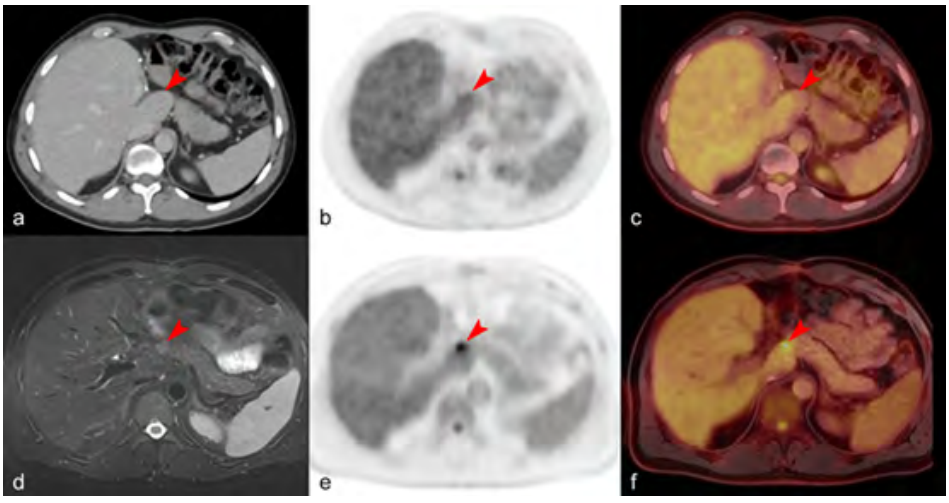

Figure 1: 65-year-old male with colon cancer metastatic to liver, with small lesion in segment 1 of the liver. The lesion is not visualized on PET or CT of PET/CT (a,b) including fused images (c). The hepatic lesion is clearly seen on PET/MR on both MR (d), PET (e), and fused PET/MR images (f).

Table 1: Pearson correlation statistics (P<0.001)

Parameter	R
SUVmean	0.89
SUVmax	0.91
TBRmean	0.9
TBRmax	0.93

SUVmean - Mean standardized uptake value; SUVmax - Maximum standardized uptake value; TBRmean - Mean tumor-to-background ratio; TBRmax - Maximum tumor-to-background ratio.

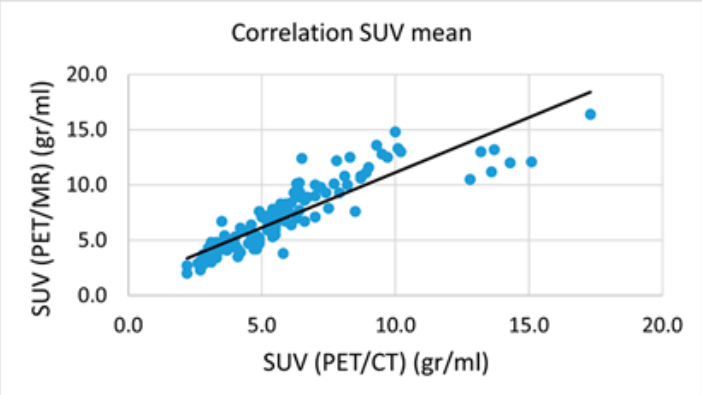

Figure 2: Correlation between SUVmean values extract from PET/CT images and from PET/MR images.
SUVmean - Mean standardized uptake value

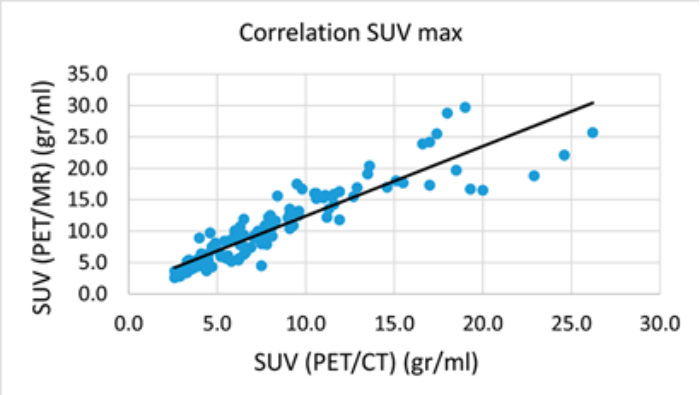

Figure 3: Correlation between SUVmax values extract from PET/CT images and from PET/MR images.
SUVmax - Maximum standardized uptake value

Table 2: Summary of numerical values extracted from Bland-Altman analysis.

Parameter	Limits of agreement span (gr/ml)	Average difference (gr/ml)	Average % difference*
SUVmean	1.1	2.8	17.9
SUVmax	2.2	4.8	23.1
TBRmean	0.5	1.9	18.5
TBRmax	0.4	1.1	18.6

* - % difference=difference*100/average SUV (or TBR).
SUVmean - Mean standardized uptake value; SUVmax - Maximum standardized uptake value; TBRmean - Mean tumor-to-background ratio; TBRmax - Maximum tumor-to-background ratio.

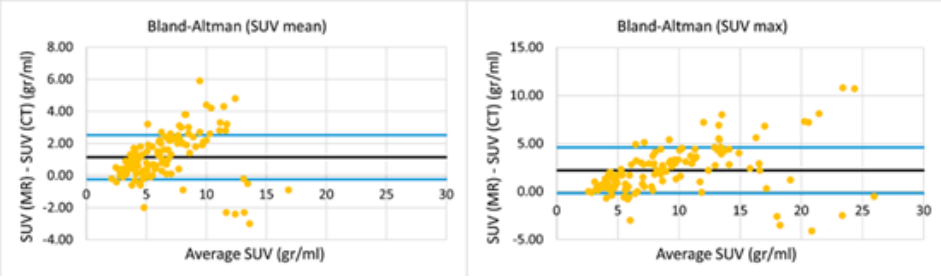

Figure 4: Bland-Altman plot for SUV: (a) SUVmean; (b) SUVmax.
SUVmean - Mean standardized uptake value; SUVmax - Maximum standardized uptake value

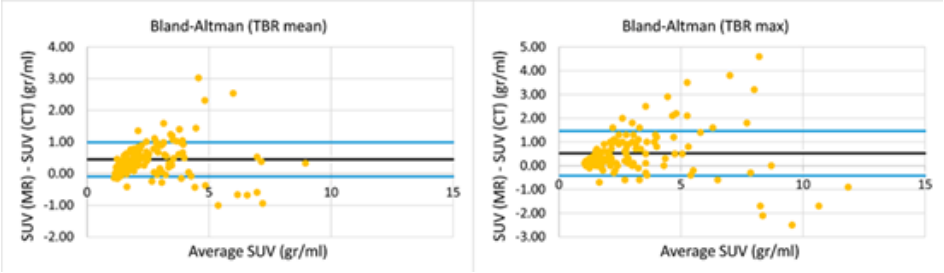

Figure 5: Bland-Altman plot for TBR: (a) TBRmean; (b) TBRmax.
TBRmean - Mean tumor-to-background ratio; TBRmax - Maximum tumor-to-background ratio

Table 3: Paired T test

SUVmean	t	9.1
	P	<0.001
SUVmax	t	10.2
	P	<0.001
TBRmax	t	6.1
	P	<0.001
TBRmean	t	9.1
	P	<0.001

SUVmean - Mean standardized uptake value; SUVmax - Maximum standardized uptake value; TBRmean - Mean tumor-to-background ratio; TBRmax - Maximum tumor-to-background ratio.

Table 4: Wilcoxon signed rank test

Parameter	Rank type	N	Mean Rank	Sum of Ranks
SUVmean_MR - SUVmean_CT	Negative Ranks	20	44.13	882.5
	Positive Ranks	109	68.83	7502.5
	Ties	2		
	Total	131		
SUVmax_MR - SUVmax_CT	Negative Ranks	15	40.97	614.5
	Positive Ranks	114	68.16	7770.5
	Ties	2		
	Total	131		
TBRmax_MR - TBRmax_CT	Negative Ranks	21	52.67	1106
	Positive Ranks	97	60.98	5915
	Ties	13		
	Total	131		
TBRmean_MR - TBRmean_CT	Negative Ranks	18	47.67	858
	Positive Ranks	113	68.92	7788
	Ties	0		
	Total	131		

SUVmean - Mean standardized uptake value; SUVmax - Maximum standardized uptake value; TBRmean - Mean tumor-to-background ratio; TBRmax - Maximum tumor-to-background ratio.

5. Discussion

Accurate treatment of hepatic metastases requires optimal imaging of lesions including smaller harder to visualize lesions, in order to determine resectability, appropriateness for ablation, neoadjuvant chemotherapy or standard chemotherapy. Imaging may be performed both before and after treatment. After treatment with chemotherapy lesions may vanish on follow up imaging as a result of chemotherapy, referred to as «disappearing liver lesions'. Whether these disappearing lesions represent a true cure (complete response) or nonvisualized residual viable tumor too small to be seen on imaging is subject to speculation. Berimani et al [11], point out that over half of disappearing liver lesions seen on contrast enhanced CT had evidence of residual tumor on surgery or follow up imaging. Even on MRI disappearing liver lesions represent a true cure in only 40-85% of cases [11].

This study compared the detection rate and quantitative PET pa-

rameters of liver metastases on PET/CT and PET/MR, with each patient being his own control. Using MR data as a gold standard PET identified 71% of the lesions on PET/CT and 76% on PET/MR. The majority of the lesions missed were lesions smaller than 2.5 cm.

In our study PET/MR detected significantly more small lesions than PET/CT. While in cases of extensive metastases this improved detection may not be of high clinical relevance. However, in cases of small lesions, minimal hepatic disease, or disappearing liver lesions PET/MR could potentially offer valuable insight.

A significantly higher uptake was detected on PET of PET/MR with SUVmean and SUVmax 17.9% and 23.1% higher on PET/MR compared to PET/CT. Likewise TBR mean and TBR max were higher on PET-MR by 18.5%and 18.6% respectively. These findings are in agreement with those reported by Demir et al [12], who concluded that PET/MR was 4 times more sensitive than PET/CT, with contrast 9% higher than PET/CT. Al-Nabhani et al [13], demonstrated 10% increase in mean SUV on PET/MR as compared to PET/CT, and Pace et al [14] reported increased SUVmax of 34% and SUVmean of 21% on PET/MR compared to PET/CT. In contradistinction, Wiesmuller [15] demonstrated decreased uptake on PET/MR compared to PET/CT, with a 22% decrease in SUVmax and a 10% decrease in SUVmean.

There are several factors that may contribute to the higher tracer uptake measured on PET of PET/MR compared to PET of PET/CT. PET/MR has a wider axial FOV and smaller ring diameter both of which can improve scanner sensitivity [11]. At our facility PET/MR has 5 detector rings, while the PET/CT has only 4 detector rings, also resulting in improved sensitivity for the PET/MR. PET/MR was focused on the liver acquiring PET data for 20 minutes compared to 4 minutes for PET-CT. This may be a limitation in study design, yet this in any case this is the acquisition protocol often used in routine clinical practice.

Overall, when comparing the anatomic portion of the PET studies (CT vs MR), MR is clearly better at defining metastatic lesions than CT. Therefore, coupling the superior anatomic resolution of MR with the superior metabolic delineation with PET of the PET/MR, leads to a more thorough evaluation of the liver, which may well alter patient management.

The difference in detection rate of relevant lesions, and the difference in FDG quantitation may create difficulty when comparing studies performed at different time points during the course of the disease, particularly if monitoring response to therapy is the indication for follow up PET study. Due consideration to performing the same study pre and post treatment may be in order.

In conclusion, while both PET/CT and PET/MR are viable options for evaluation of liver metastases, the better visualization and higher uptake of metastases on PET of PET/MR, as well as the superiority of MR in the detection of lesions make PET/MR a more sensitive modality for the detection of liver metastases. This is especially true in cases of smaller lesions. The findings of this head-to-head comparison may have an impact on both accurate staging of liver disease and monitoring response to therapy.

References

1. Weiss L, Grundmann E, Torhorst J, Hartveit F, Moberg I, Eder M, et al. Haematogenous metastatic patterns in colonic carcinoma: an analysis of 1541 necropsies. J Pathol. 1986; 150(3): 195-203.
2. Riemsma RP, Bala MM, Wolff R, Mitus JW, Pedziwiatr M, et al. Transarterial (chemo)embolisation versus no intervention or placebo intervention for liver metastases. Cochrane Database Syst Rev. 2013;(4):CD009498.
3. Mentha G, Terraz S, Andres A, Toso C, Rubbia-Brandt L, Majno P. Operative management of colorectal liver metastases. Semin Liver Dis. 2013;33 (3): 262–272.
4. Sutherland LM, Williams JA, Padbury RT, Gotley DC, Stokes B, Maddern GJ. Radiofrequency ablation of liver tumors: a systematic review. Arch Surg. 2006; 141(2): 181-190.
5. Benoist S, Nordlinger B. The role of preoperative chemotherapy in patients with resectable colorectal liver metastases. Ann Surg Oncol. 2009; 16(9): 2385-2390.
6. Namasivayam S. Imaging of Liver Metastases: MRI. Cancer Imaging. 2007; 7(1): 2-9.
7. Scharitzer M, Ba-Ssalamah A, Ringl H, Kölblinger C, Grünberger T, Weber M, et al. Preoperative evaluation of colorectal liver metastases: comparison between gadoxetic acid-enhanced 3.0-T MRI and contrast-enhanced MDCT with histopathological correlation. Eur Radiol. 2013; 23(8): 2187-96.
8. Frankel TL, Gian RK, Jarnagin WR. Preoperative imaging for hepatic resection of colorectal cancer metastasis. J Gastrointest Oncol. 2012; 3(1): 11-8.
9. Beiderwellen K, Geraldo L, Ruhlmann V, Heusch H, Gomez B, Nensa F, et al. Accuracy of [18F]FDG PET/MRI for the Detection of Liver Metastases. PLoS One. 2015; 10(9): e0137285.
10. Cheson BD. Staging and response assessment in lymphomas: the new Lugano classification. Chin Clin Oncol. 2015; 4(1): 5.
11. Barimani D, Kauppila JH, Sturesson C, et al. Imaging in disappearing colorectal liver metastases and their accuracy: a systematic review. World J Surg Oncol. 2020; 18(1): 264.
12. Demir M, Toklu T, Abuqbeitah M, Çetin H, Sezgin HS, Yeyin N, et al. Evaluation of PET Scanner Performance in PET/MR and PET/CT Systems: NEMA Tests. Mol Imaging Radionucl Ther. 2018; 27(1): 10-18.
13. Al-Nabhani KZ, Syed R, Michopoulou S, Alkalbani J, Afaq A, Panagiotidis E, et al. Qualitative and quantitative comparison of PET/CT and PET/MR imaging in clinical practice. J Nucl Med. 2014; 55(1): 88-94.
14. Pace L, Nicolai E, Luongo A, Aiello M, Catalano OA, Soricelli A, et al. Comparison of whole-body PET/CT and PET/MRI in breast cancer patients: lesion detection and quantitation of 18F-deoxyglu-

cose uptake in lesions and in normal organ tissues. Eur J Radiol. 2014;83(2):289-96.

15. Wiesmüller M, Quick HH, Navalpakkam B, Lell MM, Uder M, Ritt P, et al. Comparison of lesion detection and quantitation of tracer uptake between PET from a simultaneously acquiring whole-body PET/MR hybrid scanner and PET from PET/CT. Eur J Nucl Med Mol Imaging. 2013; 40(1): 12-21.